Study of $\pi^- p \to \omega n, \phi n$ at 2.10 BeV/c*†

J. H. Boyd,‡ A. R. Erwin, W. D. Walker, and E. West§
University of Wisconsin, Madison, Wisconsin
(Received 7 September 1967)

In a bubble-chamber experiment at 2.10 BeV/c we have determined the cross section $\sigma(\pi^- p \to \omega n) = 1.41 \neq 0.18$ mb by fitting the neutral and the charged effective-mass spectra for events of the type $\pi^- p \to \pi^+\pi^- n(m)\pi^0$, $m \geq 1$, with appropriate phase-space and resonance effective-mass distributions. Cross sections for other contributing reactions are also given. The cross section $(\pi^- p \to \phi n) = 19_{-8}^{+9}$ μb (statistical error) was obtained by using the maximum-likelihood method to determine the cross section corresponding to a peak (at the ϕ mass 1019.5 MeV) in the K^+K^- effective-mass spectrum of $K^+K^- n$ events. The relative probability of the cross section being zero is 0.07. We conclude that $\sigma(\pi^- p \to K^+K^- n)$ is between 75 and 150 μb at 2.10 BeV/c. The K-pair events studied include events both with and without a visible K decay. The nondecay-event identification procedure included a visual bubble-density estimation. We calculate an ω-ϕ mixing angle of $42.1 \pm 1.8°$ (statistical error) using a quark-model prediction by Alexander, Lipkin, and Scheck. This mixing-angle prediction agrees well with values calculated from $SU(3)$ mass formulas. The input data for this calculation are our ϕn cross section (at c.m. energy 2.20 BeV) and the ωn cross section at c.m. energy 1.96 BeV which we estimated from $\pi^+ n \to \omega p$ data.

I. INTRODUCTION

THE experimental data presented here are primarily results on the reactions

$$\pi^- p \to \omega n \tag{1a}$$

and

$$\pi^- p \to \phi n \tag{1b}$$

at 2.10 BeV/c obtained in a bubble-chamber experiment using the 14-in. Adair chamber at Brookhaven. The beam and the chamber have been described previously.[1,2]

A common result of many experiments has been the observation that the cross section observed in any ϕ production reaction is always much smaller than the cross section observed in the corresponding ω production reaction. Our cross sections for reactions (1) exhibit this behavior very strikingly. The ϕn reaction can barely be detected: $\sigma(\pi^- p \to \phi n) = 19 \pm 9$ μb (statistical error). On the other hand, the ωn cross section, $\sigma(\pi^- p \to \omega n) = 1.41 \pm 0.18$ mb (statistical error), is about 4% of the $\pi^- p$ total cross section. In Sec. V we show that the ratio of our ϕn cross section to the ωn cross section (at an appropriately chosen energy) is consistent with a prediction by Alexander, Lipkin, and Scheck[3] based upon a quark model, which relates the ratio of the ϕn and ωn production amplitudes to the ω-ϕ mixing angle. The mixing-angle prediction from the model is shown to be consistent (within errors) with the mixing angles given by $SU(3)$ mass formulas.

In Sec. III we discuss the determination of the ωn cross section mentioned above. This section also includes the cross sections obtained for other reactions contributing to the sample of $\pi^- p \to \pi^+\pi^- n(m)\pi^0$ (where $m \geq 1$) events whose charged and neutral mass spectra were studied to determine the ωn cross section. In Sec. IV we describe the search for the $\pi^- p \to K^+K^- n$ events, which were studied to determine the ϕn cross section. We observe the ϕ through its K^+K^- decay mode. The cross section was obtained by using the maximum-likelihood method to measure the size of the ϕ peak in the K^+K^- mass spectrum.

II. DATA ANALYSIS

A. Scanning and Measuring

Area scanning was used to locate events. The scanning efficiency was determined to be 91%. The muon and electron contaminations in the beam have been determined[4] by scanning for and measuring the momenta of "knock-on" electrons from beam tracks. The muon contamination is less than 6% and the electron contamination is less than 0.5%. The exact values of of the scanning efficiency and beam contaminations are not important since the cross-section determinations are normalized to total cross-section measurements from another experiment.[2]

A fiducial volume for two-prong events was chosen which resulted in beam tracks ≥ 2 cm long and in forward-going tracks ≥ 15 cm long. Events with beam tracks which did not enter the chamber with direction cosines consistent with the proper beam direction were discarded. These criteria provide an event sample of satisfactory quality to give good discrimination between the various constrainable two-prong hypotheses.

The measuring machines used included both film-plane and image-plane encoding types having a least count of 1μ on the film. A competent measurer can

* Work supported in part by the U. S. Atomic Energy Commission under Contract No. AT(11-1)-881, COO-881-120.
† Based upon a portion of a thesis submitted by J. H. Boyd in partial fulfillment of the requirements for the degree of Doctor of Philosophy at the University of Wisconsin.
‡ Now at the Illinois Institute of Technology, Chicago, Ill.
§ Now at the University of Toronto, Toronto, Canada.
[1] E. West, J. H. Boyd, A. R. Erwin, and W. D. Walker, Phys. Rev. **149**, 1089 (1966).
[2] P. H. Satterblom, W. D. Walker, and A. R. Erwin, Phys. Rev. **134**, B207 (1964).
[3] G. Alexander, H. J. Lipkin, and F. Scheck, Phys. Rev. Letters **17**, 412 (1966).
[4] G. A. Hoyer (private communication).

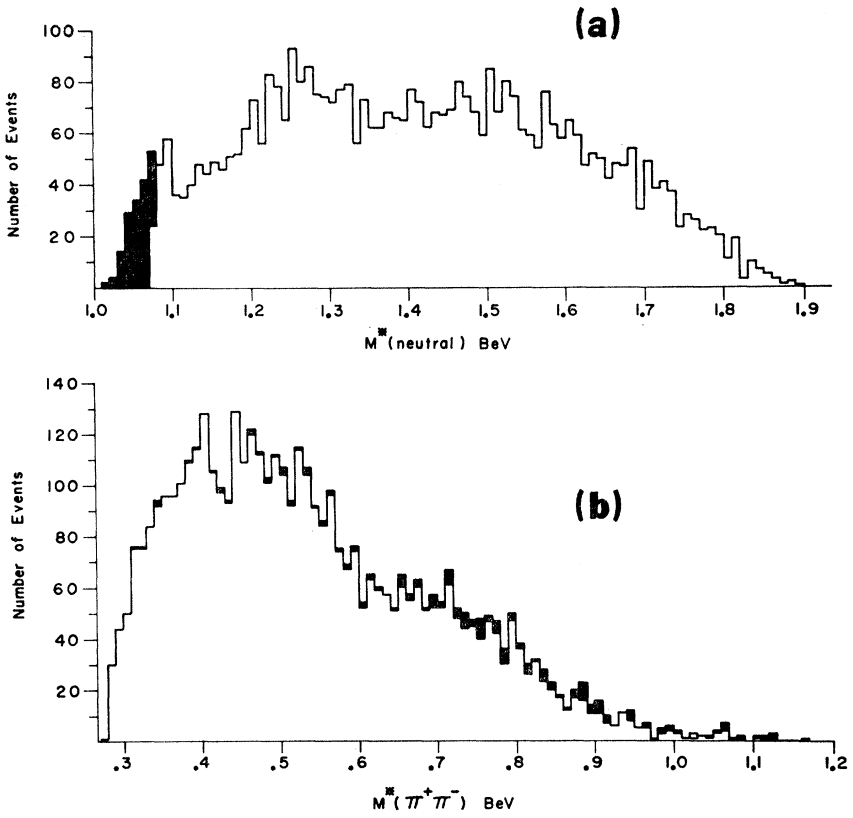

FIG. 1. (a) M^*(neutral) and (b) $M^*(\pi^+\pi^-)$ distributions from $\pi^- p \to \pi^+\pi^- n(m)\pi^0$; $m \geq 1$ events.

reset the machine on a point with about a 2- to 3-μ rms error on the film.

B. Analysis of Events

The computer event analysis system used a two-step procedure of spatial reconstruction followed by kinematic fitting. The kinematic fitting program tried the constrained hypotheses:

$$\pi^- p \to \pi^- p \tag{2a}$$
$$\to \pi^- p\pi^0 \tag{2b}$$
$$\to \pi^+\pi^- n. \tag{2c}$$

In addition to the computed values of χ^2, tests of ionization estimates, stopping track ranges, and coplanarity were used in deciding which hypothesis was correct. Events which did not fit any of the above three hypotheses were assigned to the multiple neutral production hypothesis most consistent with the observed bubble densities and the computed values for the missing mass. These hypotheses are

$$\pi^- p \to \pi^- p(m)\pi^0, \quad m \geq 2 \tag{3}$$
$$\to \pi^+\pi^- n(m)\pi^0, \quad m \geq 1. \tag{4}$$

The above procedure misclassifies strange-particle events where no visible decay is present. A portion of these misclassified events was retrieved for reclassification as described in Sec. IV.

III. $\pi^+\pi^-$ EVENTS WITH MULTIPLE NEUTRALS, INCLUDING $\pi^- p \to \omega n$

The main purpose for undertaking a study of reactions (4) was to determine the cross section for the reaction $\pi^- p \to \omega n$.

Since the branching ratio for the decay mode $\omega \to \pi^+\pi^-\pi^0$ is quite well known,[5] the cross section for reaction (4) may be determined by measuring the cross section for the reaction $\pi^- p \to \omega n$, $\omega \to \pi^+\pi^-\pi^0$. The cross sections for other reactions contributing to reactions (4) are also determined. The raw data for these cross-section determinations are the $\pi^+\pi^-$ and the neutral mass spectra for reactions (4) shown in Fig. 1.

There are 4443 events classified in the category of reactions (4). The neutral mass spectrum [Fig. 1(a)] shows a small peak of events clustered around the $\pi^0 n$ threshold, which is presumed to consist largely of misclassified $\pi^+\pi^- n$ events. In the analysis procedure to be described below all the events which had a neutral mass less than this threshold were removed from the sample, as indicated in Fig. 1. The cross section per event in this sample is[1] 1.57 ± 0.03 μb/event. Thus the total cross section for the remaining 4272 events is $\sigma(\pi^- p \to \pi^+\pi^- n(m)\pi^0) = 6.71 \pm 0.16$ mb.

[5] The branching ratio $(\omega \to \pi^+\pi^-\pi^0)/(\omega \to \text{all modes}) = 0.840 \pm 0.016$ may be calculated from the branching ratios $(\omega \to \pi^+\pi^-)/(\omega \to \pi^+\pi^-\pi^0) = 0.082 \pm 0.02$ from Ref. 8 and $(\omega \to \text{neutrals})/(\omega \to \pi^+\pi^-\pi^0) = 0.106 \pm 0.01$ from Ref. 7, assuming that no other modes contribute.

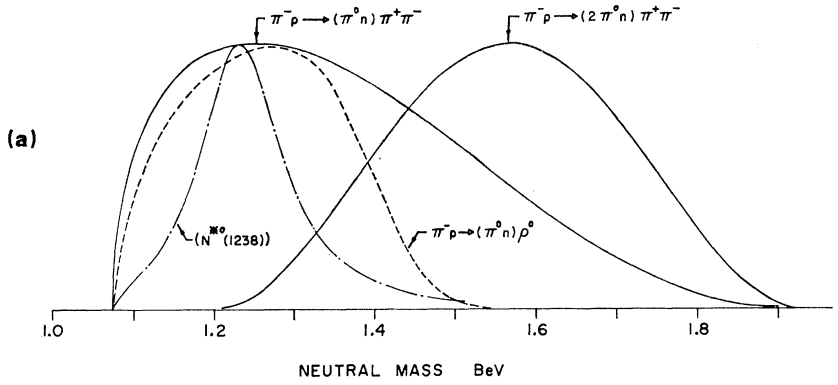

FIG. 2. Computed effective-mass spectra (arbitrary vertical scales) (a) M^* (neutral), (b) $M^*(\pi^+\pi^-)$.

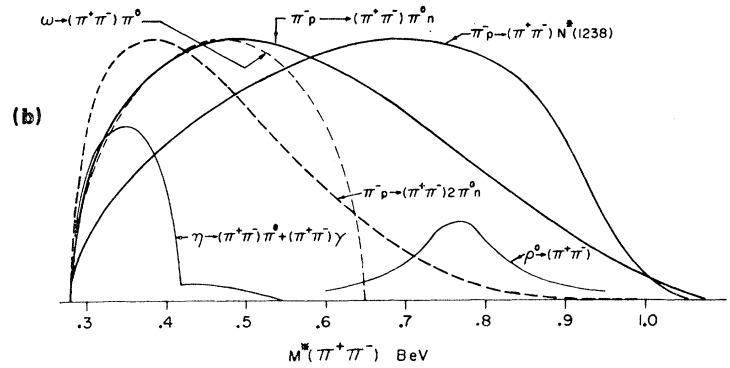

A. Contributing Reactions and Their Mass Spectra

One may obtain a qualitative idea of what to expect by examining the cross sections[2] found in the same film for reactions which have final states which differ from those below by permutation of some of the charges in the final state. However, no such related reactions exist for the final states ωn and ηn. Table I lists related four-prong reactions and their cross sections.[2] Reactions which might be expected to make significant contributions to the mass spectra being considered are

$$\pi^-p \rightarrow \pi^+\pi^-\pi^0 n \quad (5)$$

$$\rightarrow \pi^+\pi^-(2\pi^0)n \quad (6)$$

$$\rightarrow \omega n \quad (7)$$

$$\rightarrow \rho^0 N^{*0}(1238) \quad (8)$$

$$\rightarrow \rho^0\pi^0 n \quad (9)$$

$$\rightarrow N^{*0}(1238)\pi^+\pi^- \quad (10)$$

$$\rightarrow N^{*+}(1238)\pi^0\pi^-. \quad (11)$$

Among the processes which might be expected to produce smaller contributions are

$$\pi^-p \rightarrow \pi^+\pi^-(m)\pi^0 n, \quad m>2, \quad (12)$$

and reactions which produce η's, such as

$$\pi^-p \rightarrow \eta n. \quad (13)$$

Each of the reactions (5)–(13) contributes to both the charged and the neutral mass spectra. (Each reaction must of course contribute the same total area to each spectrum, since each event contributes once to each.) The shapes of the mass spectra contributions expected for reactions (5)–(13) are shown in Figs. 2–4. Since the decay products of the N^{*+} in reaction (11) contribute to both the neutral and charged mass

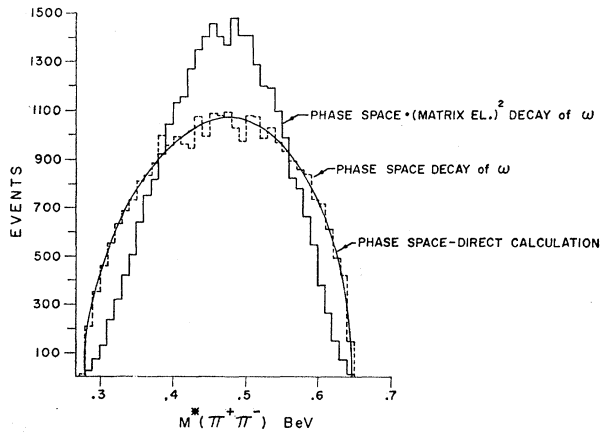

FIG. 3. $M^*(\pi^+\pi^-)$ from 30 000 Monte Carlo generated $\omega \rightarrow \pi^+\pi^-\pi^0$ decays compared to a direct phase-space calculation.

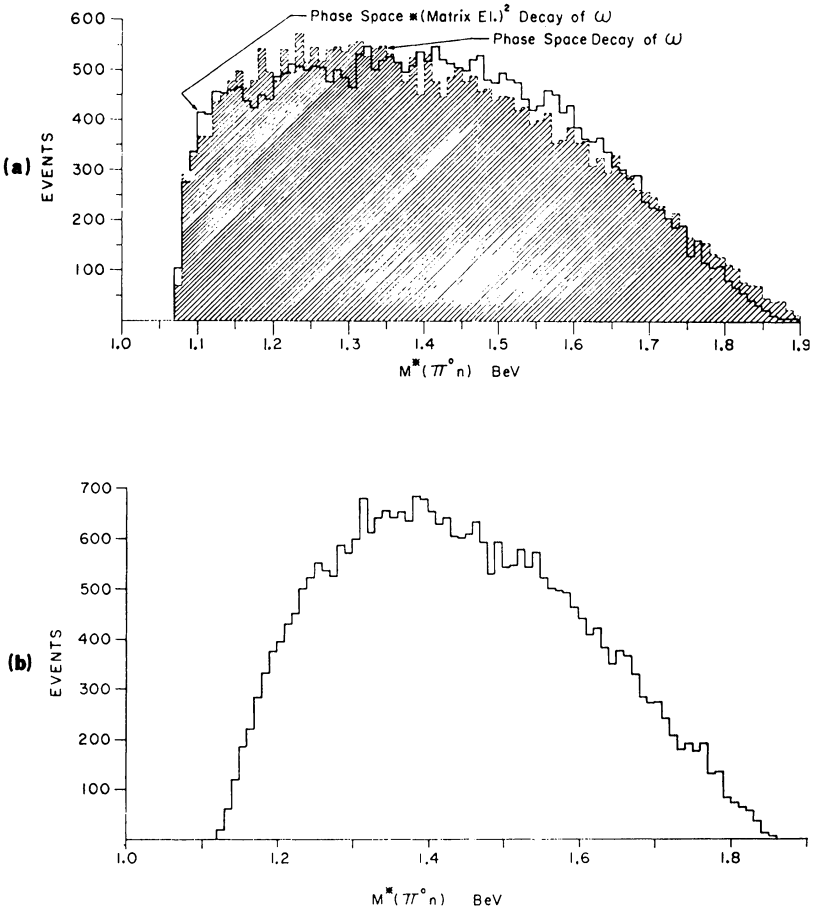

FIG. 4. (a) $M^*(\pi^0 n)$ from 30 000 Monte Carlo generated $\pi^- p \to \omega n$; $\omega \to \pi^+\pi^-\pi^0$ events. (b) $M^*(\pi^0 n)$ from 30 000 Monte Carlo generated $\pi^- p \to \eta n$; $\eta \to \pi^+\pi^-\pi^0$ events.

spectra, we have assumed that the presence of the resonance will not produce charged and neutral mass spectra which differ significantly from simple phase-space distributions. Thus we do not treat reaction (11) separately, but rather we assume that its cross section is included in that tabulated for reaction (5).

We now describe how these curves were obtained. The contributions from reactions (5) and (6) are assumed to be described adequately by simple phase-space mass distributions, as was the case in the related 4-charged-particle reactions.[2] A computer program[6] was used to calculate the phase-space mass spectra. The reactions in which a broad resonance is produced contribute more complicated spectra. For example, in computing the $\pi^+\pi^-$ mass spectrum for reaction (10), it is necessary to take account of the width of the $N^{*0}(1238)$. This effect was treated approximately by calculating the distribution for various values of "N^* mass" and adding the distributions in a weighted manner to approximate the effect of the finite N^* width.

The mass spectra from the ωn and the ηn final states are more difficult to calculate because the decay products from the resonances consist of both charged and neutral particles. Thus the particles contributing to the neutral mass come partly from the decay of the ω or η resonances. It was possible to calculate the $\pi^+\pi^-$ spectrum [shown in Fig. 2(b)] of the η decay using the

TABLE I. A comparison of 4-prong reactions previously studied to 2-prong reactions having the same number of bodies in the final state.

4-prong reaction		Related
Reaction	Cross section[a] (mb)	2-prong reaction
$2\pi^+\pi^- p$	1.67 ± 0.08	$\pi^+\pi^-\pi^0 n$
Total $2\pi^+\pi^-\pi^0 p$, of which	1.17 ± 0.06	
$\omega\pi^- p$ contributes	0.26 ± 0.04	$\omega\pi^0 n$
$\eta\pi^- p$ contributes	0.13 ± 0.05	$\eta\pi^0 n$
Remaining $2\pi^+\pi^-\pi^0 p$ is	0.78 ± 0.07	$\pi^+\pi^- 2\pi^0 n$
4-prong including an $N^*(1238)$ as $\pi^- p$ of which a sizeable part was shown to be $N^{*0}+\rho^0$	0.11 ± 0.03	$\rho^0 N^{*0}$, where N^{*0} is seen as $\pi^0 n$
$2\pi^+ 2\pi^-\pi^0 n$	≈ 0.12[b]	$\pi^+\pi^- 3\pi^0 n$
$2\pi^+ 2\pi^- 2\pi^0 n$	≈ 0.016[c]	$\pi^+\pi^- 4\pi^0 n$

[a] Reference 21.
[b] 78 events×1.49 μb/event. No error is quoted since the identification of the events is not certain.
[c] 11 events×1.49 μb/event. See Ref. b.

[6] MOFN by R. Matsen. This program computes the M-particle mass spectrum for a state (of a given total energy) containing N particles, where $2 \leq M < N \leq 7$.

TABLE II. Partial cross sections for $\pi^-p \to \pi^+ + \pi^- +$ multiple neutrals (M.E. ≡ matrix element). (Cross sections in mb.)

Fit No.	1	2	3	4	5	6	7	8	9
Decay of ω	(M.E.)^2 × (phase space)	(M.E.)^2 × (phase space)	(M.E.)^2 × (phase space)	(M.E.)^2 × (phase space)	Phase space	Phase space	Phase space	Phase space	(M.E.)^2 × (phase space)
$\pi^+\pi^-\pi^0 n$	3.85±0.11	2.60±0.19	2.48±0.23	2.76±0.41	3.85±0.13	2.45±0.22	2.44 ±0.24	2.85±0.47	2.56±0.20
$\pi^+\pi^-(2\pi^0)n$	2.06±0.10	2.28±0.11	2.34±0.12	2.26±0.16	2.08±0.11	2.23±0.11	2.23 ±0.14	2.11±0.17	2.20±0.12
$\omega + n$	0.65±0.14	1.17±0.15	1.14±0.15	1.12±0.16	0.63±0.17	1.37±0.19	1.36 ±0.21	1.35±0.21	1.19±0.15
$\rho^0 + N^*$		0.55±0.07	0.50±0.09	0.78±0.34		0.56±0.07	0.56 ±0.10	0.97±0.35	0.55±0.07
$\pi^0 n\rho^0$			0.15±0.16	−0.27±0.31			0.004±0.17	−0.39±0.31	
$\pi^+\pi^- N^*$				−0.06±0.29				−0.29±0.29	
ηn									0.10±0.07
Total of above cross sections	6.56	6.60	6.61	6.59	6.56	6.61	6.59	6.60	6.60
$\chi^2(\pi^+\pi^-)$	61.3	22.7	23.3	21.6	72.2	31.6	31.7	29.7	22.3
$\chi^2(\pi^0 n)$	45.2	20.4	19.0	20.0	43.1	20.9	20.8	21.3	18.8
Total χ^2	106.5	43.1	42.3	41.6	115.4	52.5	52.5	51.0	41.1
Constraints	30	29	28	27	30	29	28	27	28
$P(\chi^2)$	$<10^{-5}$	0.046	0.041	0.037	$<10^{-5}$	0.005	0.003	0.004	0.054

program mentioned previously.[6] This spectrum is a weighted sum for the contributions from the two decay modes

$$\eta \to \pi^+\pi^-\pi^0 \quad \text{(branching ratio 0.25)}^7$$
$$\to \pi^+\pi^-\gamma \quad \text{(branching ratio 0.055)}.$$

The mass spectra for the ωn final state were computed twice with different assumptions:

(1) simple phase-space decay of the ω, i.e., constant matrix element;

(2) phase space × (matrix element)^2.

Since the ω has spin and parity 1^-, the matrix element is proportional to[8]

$$\mathbf{P}_1 \times \mathbf{P}_2 + \mathbf{P}_2 \times \mathbf{P}_3 + \mathbf{P}_3 \times \mathbf{P}_1 = 3\mathbf{P}_1 \times \mathbf{P}_2,$$

where the vectors are the pion momenta in the ω c.m. system. The $\pi^+\pi^-$ and $\pi^0 n$ spectra were calculated for both cases with a computer program which used a Monte Carlo method. No allowance was made for possible polarization effects. The $\pi^+\pi^-$ mass spectrum was also calculated directly[6] for case (1), and compared with the distribution given by the Monte Carlo program. The $\pi^+\pi^-$ spectra are shown in Fig. 3 and the $\pi^0 n$ in Fig. 4(a). The inclusion of the matrix element produces a marked change in the $\pi^+\pi^-$ spectrum, but only minor changes in the $\pi^0 n$. The $\pi^0 n$ spectrum from the ηn state was computed in the same manner as case (1) for the ωn state by merely substituting the η mass for the ω mass in the program. This $\pi^0 n$ spectrum is shown in Fig. 4(b).

[7] A. H. Rosenfeld, A. Barbaro-Galtieri, W. H. Barkas, P. L. Bastien, J. Kirz, and M. Roos, Rev. Mod. Phys. **37**, 633 (1965).

[8] S. M. Flatté, D. O. Huwe, J. J. Murray, J. Button-Shafer, F. T. Solmitz, M. L. Stevenson, and C. Wohl, Phys. Rev. Letters **14**, 1095 (1965); Phys. Rev. **145**, 1050 (1966).

B. Method for Determination of Cross Sections for Contributing Reactions

To determine the cross sections for reactions contributing to the multiple-production sample, the $\pi^+\pi^-$ and the neutral mass spectra were fit simultaneously with sets of mass spectra corresponding to the desired reactions. Each reaction was required to contribute the same cross section to both spectra. The data and the reaction mass spectra were integrated over 50-MeV intervals (starting and ending at multiples of 50 MeV) to produce histograms which could be handled conveniently in the fitting program.

In the fits, no contributions to χ^2 were included from the regions below 300 MeV in the $\pi^+\pi^-$ mass and below 1100 MeV in the neutral mass spectra. In the $\pi^+\pi^-$ case this was merely a convenience. The region is only 20 MeV wide and all the reaction spectra which contribute near threshold behave similarly there; thus the region would not affect the fit significantly. The excluded region in the neutral mass spectrum is 25 MeV wide, and it contains some of the misclassified events mentioned previously. Since the fitting model being used makes no allowance for these spurious events, it is imperative that this region be prevented from contributing to χ^2. Since these same spurious events are spread out smoothly over the high mass end of the $\pi^+\pi^-$ spectrum, and since there are only about 70 such events (the number of excess events in the excluded region in the neutral mass spectrum), their effect on the cross sections obtained should be small.

C. Cross Sections of Contributing Reactions

The results of the fits are given in Table II. The histogram corresponding to the sum of the reaction spectra of each fit is shown in Fig. 5. The absence of a cross section entry in the table indicates that the corre-

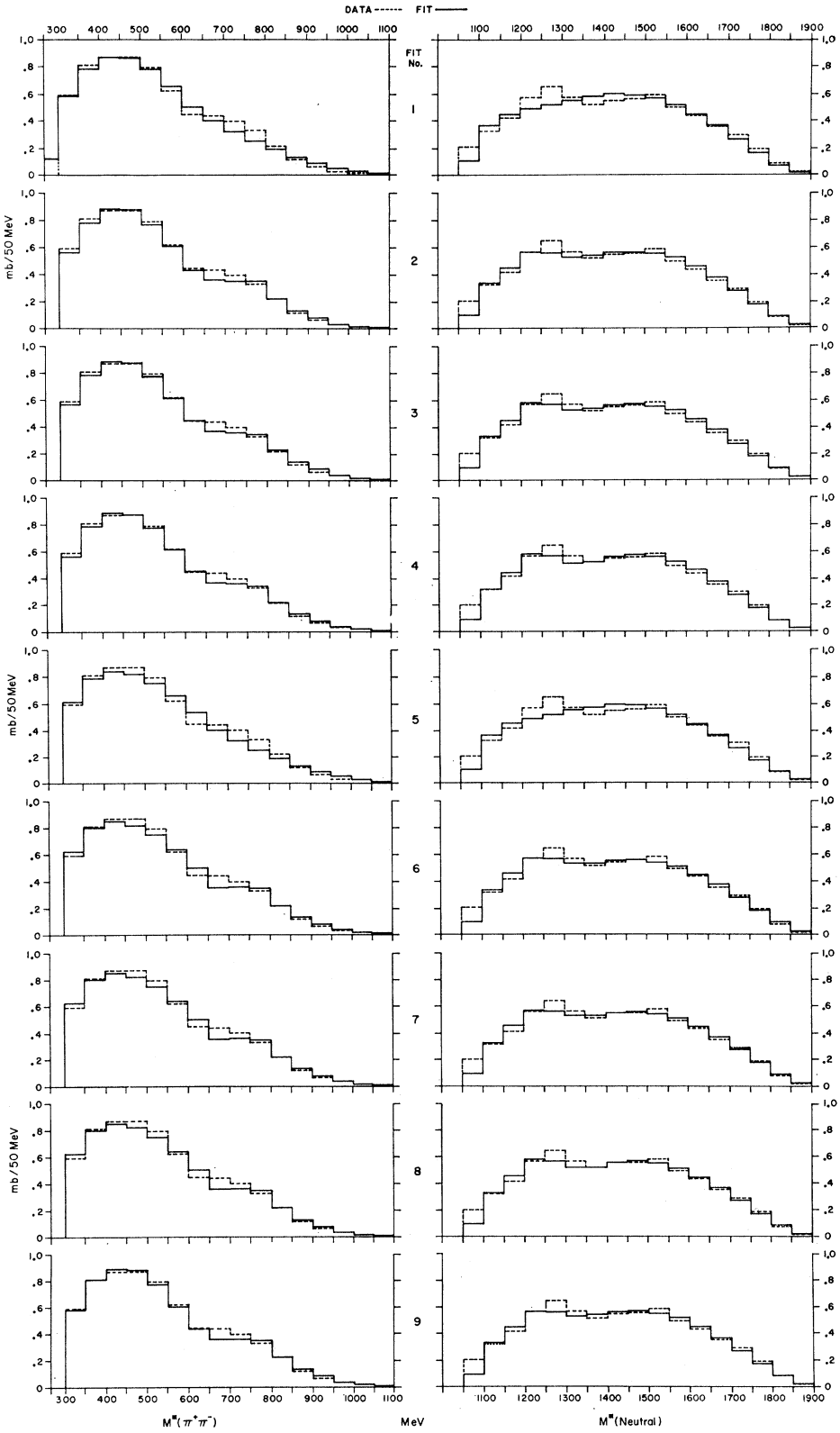

FIG. 5. Fits to effective-mass distributions from $\pi^- p \to \pi^+\pi^- n(m)\pi^0$; $m \geq 1$ events.

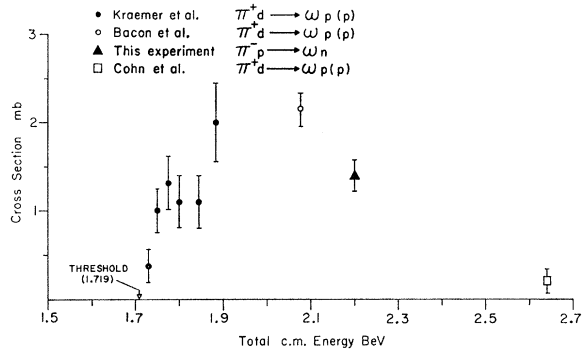

FIG. 6. Cross sections for $\pi^-p \rightarrow \omega n$ and $\pi^+p \rightarrow \omega p$. See Refs. 8–11.

sponding reaction was not included in that fit. Fits 1–4 and 9 include the correct matrix element dependence of the ω decay, whereas fits 5–8 use the phase-space approximation. The conclusions we draw from the various fits are as follows:

(a) Fits using the correct matrix element treatment of ω decay are better than the corresponding fits with the phase-space approximation.

(b) It is necessary to include the $p^0N^{*0}(1238)$ final state.

(c) Inclusion of the additional reactions in fits 3, 4, 7, and 8 does not produce statistically better fits. Furthermore, the cross sections obtained for the additional reactions are consistent with zero in every case.

(d) The ωn cross section is not sensitive to the inclusion of reactions (7), (8), and (10).

(e) Fit 9 is taken as the best representation of the data since it has the highest $P(\chi^2)$.

The ωn and ηn cross sections obtained from the fit describe only that portion of the cross sections represented by the decay modes observed.

Using the branching ratio $(\omega \rightarrow \pi^+\pi^-\pi^0)/(\omega \rightarrow \text{all modes}) = 0.840 \pm 0.016$,[5] the ωn cross section from fit 9 $\sigma(\pi^-p \rightarrow \omega n;\ \omega \rightarrow \pi^+\pi^-\pi^0) = 1.19 \pm 0.15$ mb may be converted to the total ωn cross section $\sigma(\pi^-p \rightarrow \omega n) = 1.41 \pm 0.18$ mb. The total branching ratio for the two decay modes $\eta \rightarrow \pi^+\pi^-\pi^0$ and $\pi^+\pi^-\gamma$ is 0.305 ± 0.02.[8] Using this branching ratio the ηn cross section from fit 9 $\sigma(\pi^-p \rightarrow \eta n;\ \eta \rightarrow \pi^+\pi^-\pi^0) = 0.10 \pm 0.07$ mb may be converted to the total ηn cross section $\sigma(\pi^-p \rightarrow \eta n) = 0.34 \pm 0.24$ mb.

D. Discussion

Cross sections for the charge-symmetric reaction $\pi^+n \rightarrow \omega p$ have been measured at several energies.[9–11] For comparison these values are shown with our ωn value in Fig. 6. An earlier, higher, and less precise estimate of the ωn cross section from our data (which is shown in Fig. 18 of Ref. 9) is obsolete. We note that $P(\chi^2)$ for fit 9 is only 0.054, so that for some purposes it might be desirable to scale up our errors by a factor of 1.2. [Increasing the input errors by this factor would cause the output errors to be scaled by the same factor and would give $P(\chi^2) = 0.5$.]

IV. K-PAIR EVENTS AND DETERMINATION OF $\sigma(\pi^-p \rightarrow \phi n)$

The reactions

$$\pi^-p \rightarrow K^+K^-n \tag{14}$$

and

$$\pi^-p \rightarrow K^0K^-p \tag{15}$$

are discussed in this section. The events in which a charged decay was observed (referred to as the "decay events") were identified by March.[12] This section describes the analysis of events ("nondecay events") in which no charged decay or K^0 was observed in the chamber. It proved to be impossible to obtain a clean sample of K^0K^-p nondecay events, so most of the results of this section concern the K^+K^-n events. We present evidence for the observation of the ϕ in the K^+K^- mass spectrum of the K^+K^-n events. Using the ϕ decay branching ratio information presently available,[13,14] we calculate the cross section for the reaction $\pi^-p \rightarrow \phi n$.

A. Event Identification—Nondecay Events

Events of the reactions (14) and (15) in which neither K meson decayed visibly in the chamber could not be distinguished on the scanning table from the more frequent two-charged-particle ("two-prong") reactions (2). Thus the K-pair events were put through the same analysis procedure. Since incorrect hypotheses were being tested, no satisfactory fit was obtained, and they were classified (incorrectly) as examples of the multiple production reactions (3) and (4).

K-pair events were retrieved from the multiple-pion production sample in the following manner: The missing mass was recalculated for each event for each K-pair hypothesis. The appropriate K-pair kinematic fit was attempted for each event which had a missing mass within 150 MeV of the neutron mass for the K^+K^-n hypothesis, or of the K^0 mass for the K^-K^0p case. It

[9] R. Kraemer, L. Madansky, M. Meer, M. Nussbaum, A. Pevsner, C. Richardson, R. Strand, R. Zdanis, T. Fields, S. Orenstein, and T. Toohig, Phys. Rev. **136**, B496 (1964).

[10] T. C. Bacon, W. J. Fickinger, D. G. Hill, H. W. K. Hopkins, D. K. Robinson, and E. O. Salant, in *Proceedings of the Second Topical Conference on Resonant Particles* (Ohio University, Athens, Ohio, 1965), p. 129.

[11] H. O. Cohn, W. M. Bugg, and G. T. Condo, Phys. Letters **15**, 344 (1965).

[12] R. H. March (private communication).

[13] G. W. London, R. R. Rau, N. P. Samios, S. S. Yamamoto, M. Goldberg, S. Lichtman, M. Primer, and J. Leitner, Phys. Rev. **144**, 1034 (1966).

[14] J. S. Lindsey and G. A. Smith, Phys. Rev. **147**, 913 (1966). This is in close agreement with the value $B = 0.49 \pm 0.06$ which can be calculated from the data of Ref. 13. In both cases it has been assumed that the only ϕ decay modes which contribute significantly to the total decay rate are K^+K^-, K_1K_2, and $\rho\pi$. In both experiments all other modes have rates consistent with zero.

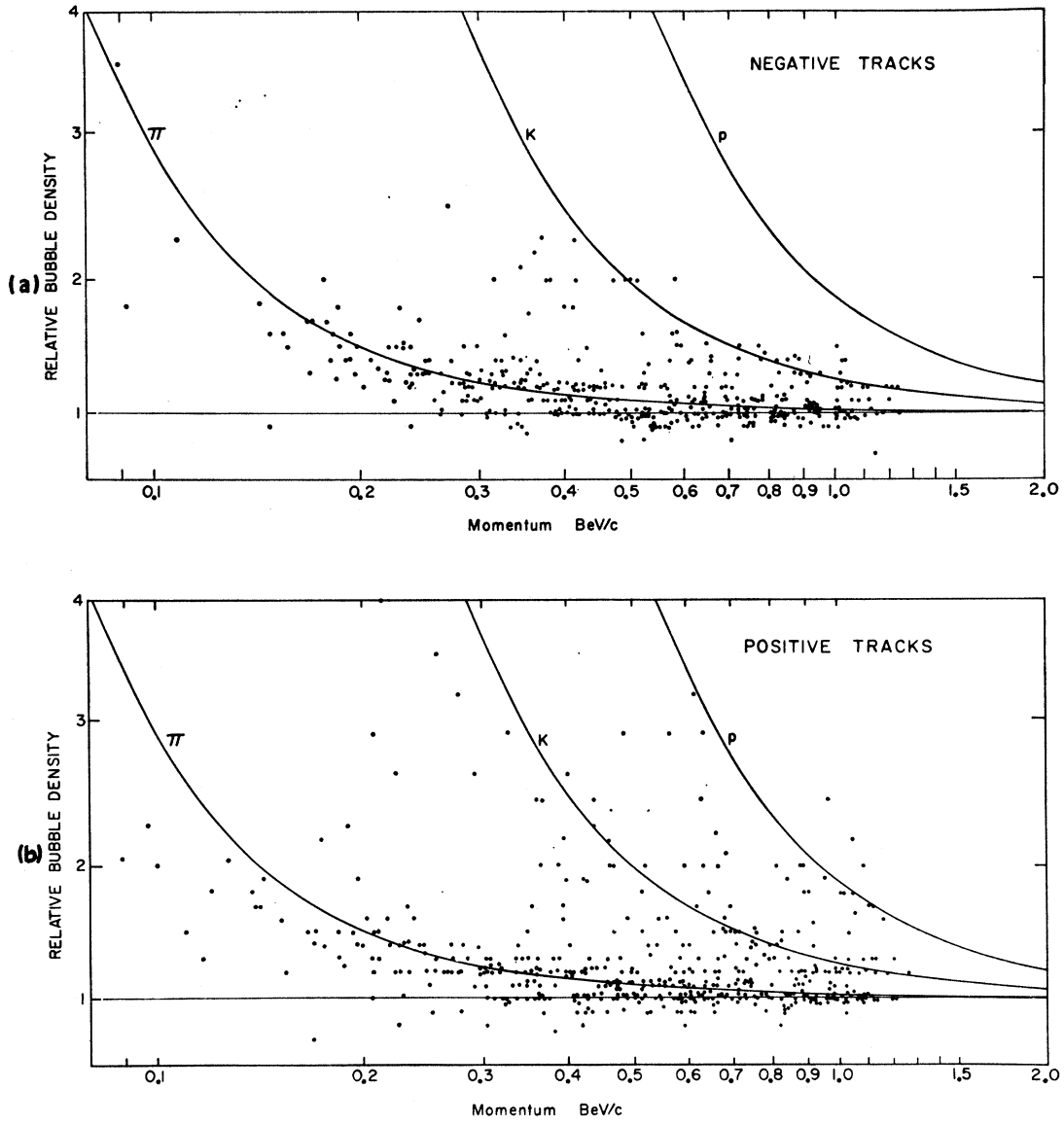

FIG. 7. Bubble-density estimates from an initial sample of K-pair candidates from the sample of $\pi^- p \to \pi^+\pi^- n(m)\pi^0$; $m \geq 1$ events. (a) Negative tracks; (b) positive tracks. The peculiar "fine structure" of the plotted points is due to the fact that the bubble-density estimates were recorded to the nearest 0.1 and that the positive and negative tracks were originally color coded on a single graph.

was necessary to consider such a large region of missing mass to be certain that all possible candidates would be included, since the missing-mass calculation used the output of the spatial reconstruction program without correcting it for energy loss. However, very few candidates were found which gave a missing mass more than 100 MeV away from the particle mass. Since each of the K-pair hypotheses has one neutral particle, the kinematic fits are 1-constraint fits. Only events with a χ^2 of less than 3.0 for one of the K-pair hypotheses were retained as possible candidates.

The final decision as to whether an event which satisfied the above criteria was indeed a K-pair event was based upon careful visual estimates of the bubble densities of the outgoing tracks relative to the bubble density of the beam track. It was required that both outgoing charged tracks be consistent with the appropriate bubble density for the momentum and mass of the particle, and that at least one K in each event be positively identified. The bubble density relative to minimum bubble density is given by[15]

$$\text{relative bubble density} = 1/\beta^2,$$

where $\beta = v/c$.

To check on the reliability of the ionization estimates, and in a sense to "calibrate" them, the initial portion

[15] V. P. Kinney, Phys. Rev. 119, 432 (1960).

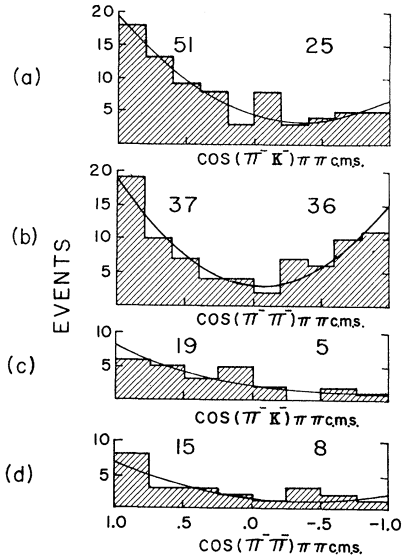

FIG. 8. $\pi\pi \rightarrow KK$ scattering angular distributions in the KK c.m. system. (The K-pair is assumed to be produced in a one-pion-exchange process.) The numbers of events in the forward and backward hemispheres are shown in the interiors of the graphs. (c.m.s. ≡ center-of-mass system.) (a) K^+K^-n events. (The curve is $4.4+6.1\cos\theta_{\text{c.m.}}+8.5\cos^2\theta_{\text{c.m.}}$.) (b) Background to K^+K^-n events. (The curve is $3.0+1.5\cos\theta_{\text{c.m.}}+14.2\cos^2\theta_{\text{c.m.}}$.) (c) K^-K^0p events. (The curve is $1.8+3.2\cos\theta_{\text{c.m.}}+2.6\cos^2\theta_{\text{c.m.}}$.) (d) Background to K^-K^0p events. (The curve is $1.8+2.4\cos\theta_{\text{c.m.}}+2.4\cos^2\theta_{\text{c.m.}}$.)

of the K-pair candidates were handled in the following manner:

The bubble density relative to the beam track was visually estimated for each track, and corrected for the perspective effect due to the dip angle. For the initial portion of candidates the bubble-density estimates were deliberately made without referring to the bubble density versus momentum curves or to the momentum information available for the event. After the bubble density had been estimated, the momentum values were looked up and the bubble-density estimate was plotted on a graph of bubble density versus momentum as shown in Fig. 7. The events shown in the figure are from reactions (4). It is apparent that a separation was achieved, and that the bubble-density estimates tended to be on the low side by an amount which increased with increasing bubble density. Note that the graph showing negative tracks shows almost no estimates falling near the proton curve.

Using this experience as a guide the remaining bubble-density estimates were done in the following manner:

Each estimate was initially made without reference to the momentum of the track. Then the estimate was compared with the possible values of bubble density at that momentum. If the estimate was in an ambiguous region, the track was carefully reexamined to see which value appeared most consistent with the track seen.

To be accepted as a K^+K^-n event, both tracks were required to be consistent with the K curve on the bubble-density graph. At least one track had to be in a momentum region where clean separation was possible. Since virtually all the candidates had at least one such track, this is not a very serious restriction, and no corrections have been made for this effect. The separation between K's and π's is believed to be good up to about 700 MeV/c; between K's and p's to about 1.3 BeV/c. At these momentum values the relative bubble densities of the two particles are about 1.5 in each case. Since the K^0K^-p events have only one charged K, it is not surprising that it proved to be impossible to reliably separate them cleanly from the far more numerous multiple-production events (which also include a proton).

To check whether the accepted samples of K-pair events could indeed be shown to be different from the rejected candidates, a background sample was made up for comparison. This sample consisted of the first rejected candidate (which had passed all tests for acceptance except the visual bubble-density estimation) following each accepted event. Thus the background events are distributed through the film in approximately the same manner as the accepted events. For one test, the angular distribution of the K pairs in the c.m. of the beam π and an assumed exchanged virtual π were computed for both the accepted and background samples. These distributions (Fig. 8) show that the K^+K^-n events have an angular distribution different from that of their background, while the K^-K^0p events are not clearly different from their background sample. The analysis of the K^-K^0p sample was discontinued at this point.

A total of 81 K^+K^-n events were found in the multiple-production samples from reactions (3) and (4). The original two-prong analysis had also produced a large class of events whose analysis had been dropped because the event did not occur in the fiducial region or because the beam particle had not entered the chamber through the thin window. Most of the data for these events had been discarded when the present analysis was undertaken. In the interest of improving the statistics of the K^+K^-n sample, the remaining portion of these abandoned events was put through the same analysis procedure described above. Fourteen additional K^+K^-n events were found and added to the sample. The total K^+K^-n cross-section normalization was determined using only the 81 events in the sample obtained previously. The cross section per event was reduced by the appropriate factor in all calculations in which the entire sample of 95 events was used. Cross sections for the K^+K^-n final state are given in part D of this section.

B. Event Identification—Decay Events

All the film for the 2.1-BeV/c exposure was scanned for strange-particle events containing a charged decay.

Such events were classified by March.[12] The decay vertex was required to fit an appropriate decay hypothesis, and the main vertex was required to fit a production hypothesis consistent with the decay observed. Bubble-density estimates were also used to verify particle identification. In this manner 19 events were found which were classified K^+K^-n. There were also 6 events in which the K^- track decayed, and which were ambiguous between K^+K^-n and K^0K^-p. In two of these events there were possible ambiguities with other hypothesis as well. These ambiguous events do not happen to affect the cross-section determination for the ϕn final state because none of these 6 events has a KK mass near the ϕ mass. For purposes of total K^+K^-n cross-section estimation, 3 of these events have been assumed to be K^+K^-n events. The cross-section estimates are discussed in part D of this section.

C. Detection Efficiency

In calculating cross sections in the K^+K^-n sample, the contribution from each event was weighted by the reciprocal of its detection probability. The detection probability for a nondecay event is the fraction of events having identical production vertices in which neither track would decay inside the illuminated region. For a decay event the detection probability is the fraction of events in which at least one track would decay inside the illuminated region. Most K's leave the illuminated region before decaying; thus the detection probabilities for the decay events are smaller than those for the nondecay events.

D. Total $\pi^- p \to K^+K^-n$ Cross Section

There were 19 events in the unambiguous K^+K^-n decay event sample. When corrected for detection efficiency they are equivalent to 182 ± 49 events (of 100% detection probability). Scaling this to include 3 ambiguous events gives 211 ± 57 events. The cross section per event for the entire chamber, and for the total film sample is 0.45 μb/event.[4] Thus the total K^+K^-n cross section as calculated from the decay events is $\sigma(\pi^- p \to K^+K^-n) = 95\pm26$ μb.

The cross section per event in the two-prong event sample from which the 81 nondecay events were extracted is 1.57 ± 0.03 μb/event.[1] When scaled to include all 95 events, this becomes 1.33 ± 0.03 μb/event. When corrected for detection efficiency the 95 events are equivalent to 104 ± 11 events. Thus the total K^+K^-n cross section as calculated from the nondecay events is $\sigma(\pi^- p \to K^+K^-n) = 139\pm14$ μb. The error quoted is the statistical error. Neither the cross section nor the error have been changed to include any systematic error estimates.

It is extremely difficult to make any reliable estimate of the systematic effects such as might be caused by the inclusion or exclusion of events due to the uncertainties in the bubble-density estimates of the nondecay events. The class of events which is most subject to error due to this cause is that in which the positive track has a high momentum since the bubble densities corresponding to the 3 possible masses are least dissimilar in this region. The laboratory momentum distribution of the K's of both the decay and the nondecay events are shown in Fig. 9. Each decay event is shown weighted by the reciprocal of its detection probability. (The events which have K^+K^- masses within 6 MeV of the ϕ mass are shown shaded. The evidence for ϕ production is discussed in part F of this section.) The K^- momentum spectrum of the nondecay events tends to be concentrated more toward the high end than that of the decay events. This is taken as an indication that some bias does exist and that it is probably in the nondecay sample. We believe that the systematic effects in the cross section determined from the nondecay events are probably at least as large as the statistical error quoted previously. We choose not to attempt to combine the two cross-section estimates, but rather to note that they seem to be in reasonable agreement and that they

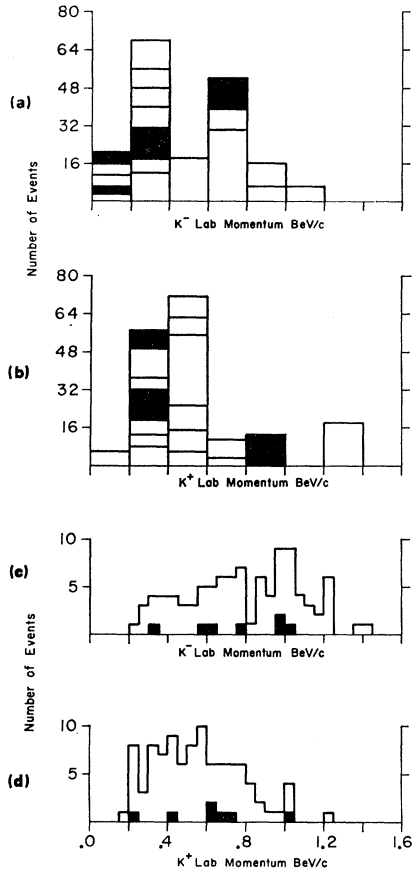

FIG. 9. Laboratory momentum spectra. Shaded events contribute to the ϕ region: $1.013 < M^*(K^+K^-) < 1.025$ BeV. (a) K^- and (b) K^+ spectra from 19 decay K^+K^-n events (weighted for detection probability). (c) K^- and (d) K^+ spectra from 95 nondecay K^+K^-n events.

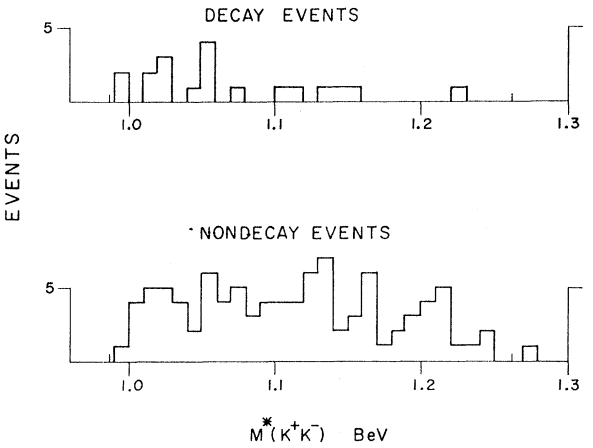

FIG. 10. Histograms of $M^*(K^+K^-)$ from $\pi^-p \to K^+K^-n$ events: (a) decay events; (b) nondecay events.

indicate that the K^+K^-n cross section is on the order of 75 to 150 μb at this energy.

Other experiments which have produced measurements of the cross section for the reaction $\pi^-p \to K^+K^-n$ include the experiment of Miller *et al.*[16] at 2.7 BeV/c which gave a cross section of 84 ± 47 μb, and the experiment of Hess *et al.*[17] which gave cross sections of 39 ± 10 μb in the region 1.58–2.3 BeV/c and 195 ± 60 μb in the region 2.9–3.3 BeV/c.

E. Mass Spectra of the K^+K^- Events

Since the weights assigned to events vary due to their different detection probabilities, it is easier to interpret the mass spectra when shown as ideograms. The K^+K^- mass distributions of both types of events are shown in histograms (Fig. 10) and ideograms (Fig. 11). In the ideograms each event is represented by a Gaussian centered at its computed mass. Its standard deviation is the computed mass error, and its area is the cross section represented by that particular event; i.e., the cross section per event multiplied by the reciprocal of the detection probability of the event. The simple phase-space mass distribution shown on each ideogram is normalized to the area of the ideogram. Two features are present in both K^+K^- ideograms: a narrow peak at the ϕ mass and a broader peak at about 1058 MeV. These features are discussed in parts F and G of this section. Ideograms of the K^+n and K^-n masses for both the decay and the nondecay events are shown in Figs. 12 and 13. There appear to be no particularly significant effects in these spectra.

F. ϕn Cross-Section Determination

Since both the decay and the nondecay K^+K^-n event samples show sharp K^+K^- mass peaks at the

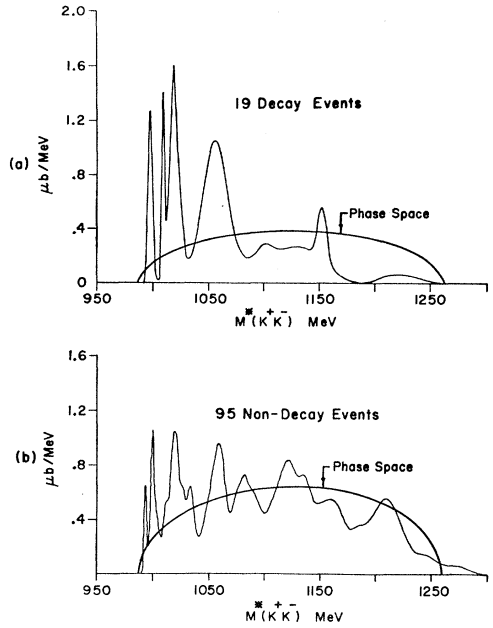

FIG. 11. Ideograms of $M^*(K^+K^-)$ from $\pi^-p \to K^+K^-n$ events: (a) decay events; (b) nondecay events.

mass of the ϕ, we presume that we observe the reaction

$$\pi^-p \to \phi n, \quad \phi \to K^+K^-. \tag{16}$$

To compute the cross section for this reaction a maximum-likelihood calculation[18] was performed. Separate likelihood functions were computed for the decay and the nondecay samples. These functions were then multiplied together to obtain the combined likelihood function. The calculation of these functions is described in the Appendix. The likelihood functions in Fig. 14 have been scaled to unit height and have been broadened

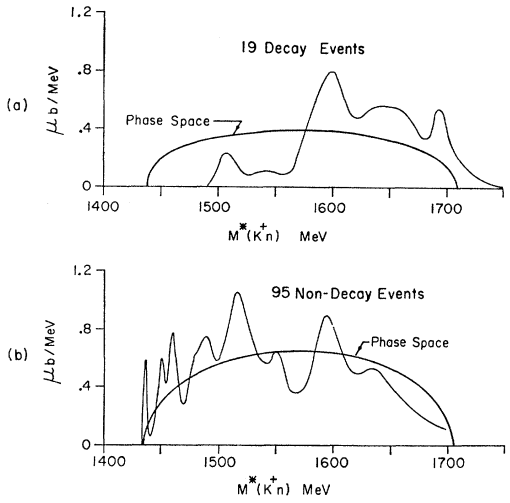

FIG. 12. Ideograms of $M^*(K^+n)$ from $\pi^-p \to K^+K^-n$ events: (a) decay events; (b) nondecay events.

[16] D. H. Miller, A. Z. Kovaca, R. McIlwain, T. R. Palfrey, and G. W. Tautfest, Phys. Rev. **140**, B360 (1965).

[17] R. I. Hess, O. I. Dahl, L. M. Hardy, J. Kirz, and D. H. Miller, Phys. Rev. Letters **17**, 1109 (1966).

[18] J. Orear, University of California Lawrence Radiation Laboratory Report No. UCRL-8417 (unpublished).

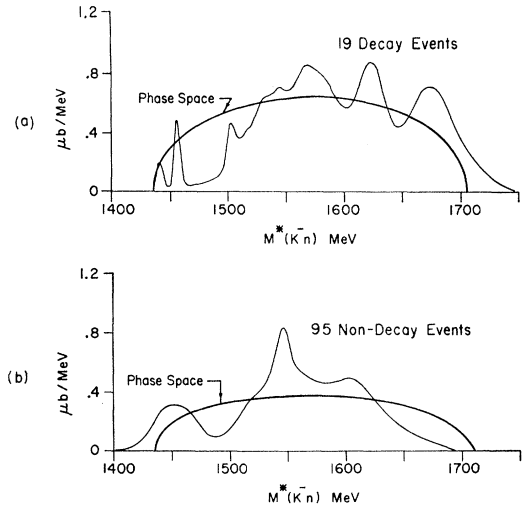

FIG. 13. Ideograms of $M^*(K^-n)$ from $\pi^- p \to K^+K^-n$ events: (a) decay events; (b) nondecay events.

by a factor (described in the Appendix) which corrects for the effect of the varying detection efficiencies of the events. The cross section obtained is $\sigma(\pi^- p \to \phi n; \phi \to K^+K^-) = 9.0_{-4.0}^{+4.5} \mu$b. The relative likelihood of the cross section being zero is 0.07. The likelihood function is slightly skewed to the high cross-section side, and its tails do not fall off as rapidly as those of a Gaussian distribution.

The average height of the background in the same region is also determined at the same time as the resonance cross section because of the manner in which the normalization was handled. The average backgrounds obtained were

$$0.37\ \mu\text{b/MeV} \quad \text{(nondecay events)}$$

and

$$0.25\ \mu\text{b/MeV} \quad \text{(decay events)}.$$

That these are reasonable values may be seen by comparing them to the values of phase space in the same region. (See Fig. 11.) Reruns of the likelihood calculations for narrower regions (still centered at the ϕ mass) showed the result to be insensitive (within the more limited statistics which then result) to the width of the region used.

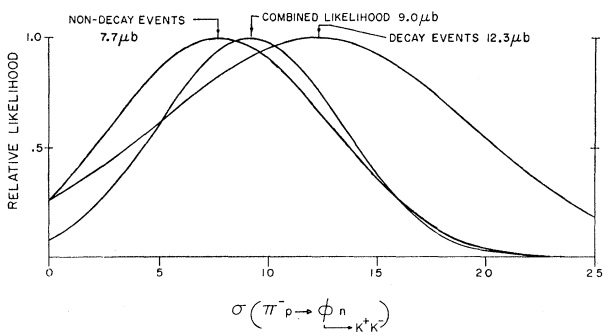

FIG. 14. Relative likelihood versus $\sigma(\pi^- p \to \phi n; \phi \to K^+K^-)$.

To check that the observed peak was centered on the ϕ mass, the calculations were repeated with the location of the resonance changed to various values in the region around the ϕ mass. The maximum value for the resonance cross section results when the resonance is placed at the ϕ mass, as shown in Fig. 15. To calculate the total cross section for the reaction $\pi^- p \to \phi n$ from our data, it is necessary to use the branching ratio[14] $B = (\phi \to K^+K^-)/(\phi \to \text{all modes}) = 0.48 \pm 0.04$, since our observation of the ϕ is by means of its K^+K^- decay mode. Using this value for B, the total ϕn cross section is $\sigma(\pi^- p \to \phi n) = 19_{-8}^{+9}\ \mu$b. This may be compared to the results of Hess *et al.*,[17] which include values of $29 \pm 15\ \mu$b in the region 1.58–1.71 BeV/c and $30.0 \pm 8.0\ \mu$b in the region 1.8–2.2 BeV/c. Their results are based on an analysis of 84 K^+K^-n decay events in the momentum interval 1.58–2.2 BeV/c.

G. Peak at $M^*(K^+K^-) = 1058$ MeV

The peak at 1058 MeV which appears in both K^+K^- mass spectrum ideograms was studied to determine whether it might be due to the $S^*(1068)$ ($I=0$, $C=P=G=+1$) observed in an experiment at 6 BeV/c by Crennell *et al.*[19] They report a width $\Gamma = 80 \pm 15$ MeV. A maximum-likelihood calculation similar to that described above gave the following cross section and widths assuming the peak at 1058 MeV to be due to a resonance

$$\sigma = 7 \pm 6\ \mu\text{b}, \quad \Gamma = 3 \pm 5 \text{ MeV (nondecay events)},$$
$$\sigma = 33 \pm 16\ \mu\text{b}, \quad \Gamma = 8 \pm 3 \text{ MeV (decay events)}.$$

Although the peak in our data is located reasonably close to that reported for the S^* (1068±10 MeV), the

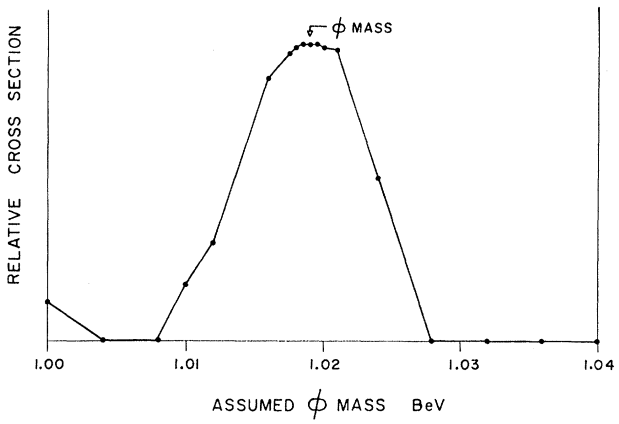

FIG. 15. Relative cross section $\sigma(\pi^- p \to \phi n; \phi \to K^+K^-)$ from maximum-likelihood calculations run with various masses assumed for the ϕ.

[19] D. J. Crennell, G. R. Kalbfleisch, K. W. Lai, J. M. Scarr, T. G. Schumann, I. O. Skillicorn, and M. S. Webster, Phys. Rev. Letters **16**, 1025 (1966).

width of the peak in our data would seem to be clearly different. As pointed out by Crennell *et al.*,[19] the $K_1^0K_1^0$ mass spectra of Erwin *et al.*[20] and Alexander *et al.*[21] show no detectable peak in this region. There is thus no convincing argument for associating the bump we observe with the S^*.

H. Discussion

The weakest point in the analysis of the K^+K^-n data is the reliance upon visual bubble-density estimates in the identification of the events. Even though reasonable care was used in making these estimates [they were all done by one of us (J. H. Boyd) and performed at an average rate of 1 event per 5 min], some biasing effects probably were introduced at this point. We have no effective way to estimate the magnitude of these effects, except to note that the approximate agreement of the total cross-section estimates from the decay and the nondecay events indicates that they are not so severe as to negate the value of the data.

In spite of the identification difficulties mentioned above, the presence of the peak at the ϕ mass in the K^+K^- mass spectrum of both the decay and the nondecay sample indicates that the reaction $\pi^-p\to\phi n$ has been observed, although with rather limited statistical significance: The ϕ peak is about 2.4 standard deviations above background.

V. CALCULATION OF THE ω-ϕ MIXING ANGLE USING A QUARK-MODEL PREDICTION

In this section we use our $\pi^-p\to\phi n$ cross section (19 ± 9 μb at total c.m. energy $E^*=2.20$ BeV) and an estimate (from Fig. 6) of the $\pi^-p\to\omega n$ cross section at the appropriately related energy (2.1 ± 0.5 mb at $E^*=1.96$ BeV) to calculate the ω-ϕ mixing angle γ, using a prediction derived by Alexander, Lipkin, and Scheck[3,22] from a quark model. Since the actual mixing angle can be calculated from $SU(3)$ mass formulas[23] (37.5° from the linear mass formula or 40.2° from the quadratic mass formula), the calculation of the mixing angle using the prediction is a test of the model. Our calculation gives a value for the mixing angle which is in the same range as the above $SU(3)$ values, thus indicating that this prediction of the model is satisfactory for the reactions considered.

The ω and ϕ mesons have $I=0$ and have the same spin and parity (1^-). In the $SU(3)$ symmetry scheme, there is an $I=0$ member ω_8 of the unitary octet and an $I=0$ unitary singlet ω_1. They may be orthogonal linear combinations of the physically observed ϕ and ω: The mixing angle γ is defined by[24]

$$\phi=\omega_8\cos\gamma-\omega_1\sin\gamma$$

and

$$\omega=\omega_8\sin\gamma+\omega_1\cos\gamma,$$

where ϕ and ω are the physically observed states.

The model[3] predicts a relation between the mixing angle and the ratios of the transition amplitudes for various two-body meson-baryon reactions. In this model it is assumed that a meson is a bound quark-antiquark system, but no assumptions regarding the structure of the baryon are necessary. It is also assumed that the transition amplitude for any meson-baryon reaction is the sum of the constituent quark-baryon and antiquark-baryon scattering amplitudes. From these assumptions, the relations

$$\frac{\langle\pi^-p\,|\,\phi n\rangle}{\langle\pi^-p\,|\,\omega n\rangle}=\frac{\langle\pi^+p\,|\,\phi N^{*++}\rangle}{\langle\pi^+p\,|\,\omega N^{*++}\rangle}=\frac{\cos\gamma-(2\sin\gamma)^{1/2}}{\sin\gamma+(2\cos\gamma)^{1/2}}=R \quad (17)$$

may be derived.[3,22] It is possible, according to Lipkin,[25] to derive Eq. (17) under less restrictive conditions if one makes more detailed assumptions about the production process (i.e., assume ρ exchange). The relation between the transition amplitude for a two-body reaction $\langle ab\,|\,a'b'\rangle$ and the cross section $\sigma(ab\to a'b')$ is[26] $|\langle ab\,|\,a'b'\rangle|^2=F\sigma(ab\to a'b')$, where the factor F is given by

$$F=E^{*2}P_i^*/P_f^*.$$

The c.m. quantities E^*, P_i^*, and P_f^* are the total energy and the initial and final momenta, respectively. We follow Meshkov, Snow, and Yodh[27] in assuming that the ratio R should be calculated using data chosen so that the transition amplitudes used are measured at energies having the same Q value in the final state, where $Q=E^*-M_{a'}-M_{b'}$. (This choice superimposes the thresholds of the reactions, which is certainly necessary.) Thus our ϕn cross section at $E^*=2.20$ BeV must be used in conjunction with the ωn cross section at 1.96 BeV. Thus

$$|R|=\left(\frac{\sigma F(\phi n \text{ at } 2.20 \text{ BeV})}{\sigma F(\omega n \text{ at } 1.96 \text{ BeV})}\right)^{1/2}=1.253\left(\frac{\sigma_{\phi n}}{\sigma_{\omega n}}\right)^{1/2}.$$

If R were zero, γ would be

$$\gamma_0=\sin^{-1}(\sqrt{\tfrac{1}{3}})=35.3°.$$

[20] A. R. Erwin, G. A. Hoyer, R. H. March, W. D. Walker, and T. P. Wangler, Phys. Rev. Letters **9**, 34 (1962).
[21] G. Alexander, O. I. Dahl, L. Jacobs, G. R. Kalbfleisch, D. H. Miller, A. Rittenberg, J. Schwartz, and G. A. Smith, Phys. Rev. Letters **9**, 460 (1962).
[22] H. J. Lipkin and F. Scheck, Phys. Rev. Letters **16**, 71 (1966).
[23] A. J. Macfarlane and R. H. Socolow, Phys. Rev. **144**, B1194 (1966).
[24] J. J. Sakurai, Phys. Rev. Letters **9**, 472 (1962); S. L. Glashow, *ibid.* **11**, 48 (1963).
[25] H. J. Lipkin (private communication).
[26] R. P. Feynman, *Theory of Fundamental Processes* (W. A. Benjamin, Inc., New York, 1962), p. 73.
[27] S. Meshkov, G. A. Snow, and G. B. Yodh, Phys. Rev. Letters **12**, 87 (1964).

The ratio R would be zero if the ϕ were a linear combination containing only strange quarks and if the ω were an orthogonal linear combination containing only nonstrange quarks coupled to isospin zero.[28]

R may be reexpressed in terms of the difference $(\gamma-\gamma_0)$ as

$$R=-\tan(\gamma-\gamma_0).$$

Since only R^2 can be determined from cross-section measurements, we are limited to determining $\gamma-\gamma_0$ from

$$|R|=|\tan(\gamma-\gamma_0)|.$$

We obtain

$$|\tan(\gamma-\gamma_0)|=1.253\left(\frac{19\pm9\ \mu\text{b}}{2.1\pm0.5\ \text{mb}}\right)^{1/2}=0.119\pm0.025.$$

Thus $|\gamma-\gamma_0|=6.8\pm1.8°$, where the error quoted includes statistical effects only. If it is assumed that $\gamma-\gamma_0$ is positive this gives a mixing angle of $42.1\pm1.8°$, which is in good agreement with the mixing angles mentioned previously. Hess *et al.*[17] obtain a value of 30 ± 8 μb for the ϕn cross section in the region 1.8–2.2 BeV/c. This gives $|\gamma-\gamma_0|=8.5\pm1.5°$, which is not in violent disagreement with the $SU(3)$ possibilities.

Lai and Schumann[29] obtained $\gamma=35.3\pm7°$ using data corresponding to the second term in Eq. (17). They obtained $|\gamma-\gamma_0|<7°$ since the data[30] for $\sigma(\pi^+p\to\phi N^{*++})$ only set an upper limit (0.01 mb at $E^*=2.78$ BeV) on the cross section.

The results of our calculation must be qualified by the following considerations:

(1) The ωn cross section used is an estimate from data for the charge symmetric reaction $\pi^+n\to\omega p$.

(2) The error quoted for the ϕn cross section includes statistical effects only. Possible systematic effects could not be ruled out.

ACKNOWLEDGMENTS

We are grateful to Professor R. W. Hartung who provided a preliminary version of his spatial reconstruction—kinematic fitting program DIANA, to Dr. M. A. Thompson who assisted in adapting it to our use, and to Professor R. H. March for providing his kinematic subroutine FIT. We wish to thank G. A. Hoyer for his extensive work on the beam, R. M. Morse for his assistance in the preparation of the data, the scanning and measuring staff of the Walker-Erwin group, and the University of Wisconsin Computing Center on whose CDC 3600 and 1604 computers the data were processed.

[28] Reference 22 and references therein.
[29] K. W. Lai and T. G. Schumann (to be published).
[30] G. H. Trilling, J. L. Brown, G. Goldhaber, S. Goldhaber, J. A. Kadyk, and J. Scanio, Phys. Letters **19**, 427 (1965).

APPENDIX: MAXIMUM-LIKELIHOOD ANALYSIS

The maximum-likelihood method[18] permits the determination of the most probable value of a parameter σ given: (1) a distribution function $f(\sigma,x)$ which describes the relative frequency of various values of some observable quantity x as a function of the parameter σ; and (2) a set of observed values of x. For our purposes σ is the cross section for reaction (16), and x is the K^+K^- mass of an event. The relative likelihood of two different values of σ is given by

$$R=\frac{\mathfrak{L}(\sigma_1)}{\mathfrak{L}(\sigma_2)}=\prod_{j=1}^{n} f(\sigma_1,x_j)/\prod_{j=1}^{n} f(\sigma_2,x_j),$$

where x_j is the value of x for event j. It is assumed here that all events have equal weight. In our case this is not so, due to the varying detection probability. The correction for this effect is discussed subsequently.

Each of the distribution functions which were compared (see Fig. 16) consisted of an energy-independent background term plus a noninterfering Breit-Wigner resonance distribution at the ϕ mass. Each distribution $f(\sigma_i,x)$ was normalized to the cross section represented by the events which occurred in a region 50 MeV wide, centered at the ϕ mass 1019.5 MeV.[7] The width used for the ϕ was $\Gamma=3.3$ MeV.[7] The K^+K^- mass errors in this region range from 1 to 8 MeV, with most being near 3 MeV. To include the effects of both the width of the ϕ and the mass error of the event, the overlap of each event with the ϕ resonance was computed by calculating the integral of a product of a Gaussian G_j (representing event j) and a Breit-Wigner resonance curve B (representing the ϕ). Both B and G_j have unit area. A given event j then contributes a factor f_{ij} to the likelihood function of a given cross section σ_i given by

$$f_{ij}=f(\sigma_i,x_j)=y_i+\sigma_i\int G_jB\,dm,$$

where y_i is the height of the background corresponding to a supposed resonance cross section σ_i. The limits for the integral were arbitrarily chosen to be 20 MeV above and below the ϕ mass.

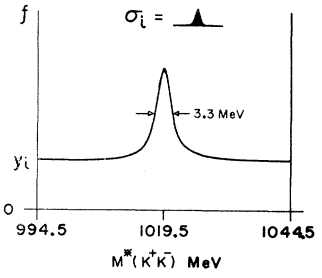

FIG. 16. Distribution function $f(\sigma_i,x)$.

When modified to include the effect of the unequal weighting of the events, the unnormalized likelihood function for a given σ_i is

$$\mathfrak{L}(\sigma_i)=\prod_{j=1}^{n}(f_{ij})^{w_j},$$

where the weight of the given event w_j is the reciprocal of the detection probability of the event, and n is the total number of events in the region. The resulting likelihood function correctly locates the most probable value of σ, but its width will be too narrow by a factor

$$[(\sum_{j=1}^{n} w_j^2)/n]^{1/4},$$

since the inclusion of the weights of the events in the manner described has artificially narrowed the likelihood function to a width appropriate to a number of events $\sum_{j=1}^{n} w_j$, rather than to the actual number n.

PHYSICAL REVIEW VOLUME 166, NUMBER 5 25 FEBRUARY 1968

K^+-Meson Production in p-p Collisions at 2.5–3.0 GeV *

W. J. HOGAN,† P. A. PIROUÉ, AND A. J. S. SMITH
Palmer Physical Laboratory, Princeton University, Princeton, New Jersey
(Received 24 August 1967)

Differential cross sections as a function of momentum are presented for the production of K^+ mesons in p-p collisions at incident proton energies of 2.54, 2.88, and 3.03 GeV. The measurements were made at 20°, 30°, and 40° relative to the direction of the internal proton beam of the Princeton-Pennsylvania accelerator. At 2.54 GeV, the results follow closely the predictions from phase space (with 60% $K^+\Sigma N$ and 40% $K^+\Lambda p$ in the final state). At 2.88 and 3.03 GeV, however, there is a definite disagreement with phase space. The data are compared to the predictions of three models: (1) a model based on the assumption that K's are produced via $p+p\rightarrow K^++X^+$, where X^+ is a $B=2$, $S=-1$ resonance which decays into a nucleon+hyperon; (2) the isobar model; and (3) the one-pion-exchange model. Model (1) is found to be inconclusive, model (2) is inadequate, and model (3) is partly successful in predicting total cross sections, but not in interpreting the *detailed* experimental observations.

I. INTRODUCTION

IN this paper we present the results of an experimental study of K^+-meson production in p-p collisions at 2.5–3.0 GeV. One of the objectives of this study was to investigate a departure from phase space which had been noticed previously[1] in the momentum distribution of K^+ mesons produced at 30° in the laboratory by 2.9-GeV protons striking a beryllium target. One of us (P. A. P.) speculated[2] that this effect could be attributed to a resonance with baryon number 2 and strangeness -1 at a mass of about 2.36 GeV/c^2. Another objective was the determination of K^+-production cross sections in this energy range to an accuracy sufficient to permit a comparison with various theoretical models.

Previous data on strange-particle production in p-p interactions at $\sim$3 GeV come, apart from very early measurements,[3] from a bubble-chamber experiment by Louttit *et al.*,[4] and a counter experiment by Melissinos *et al.*[5] The bubble-chamber data, although of limited statistical accuracy, are most useful in giving an estimate for the relative contribution of the different channels leading to a K^+ in the final state, i.e., $K^+\Lambda p$, $K^+\Sigma N$, and $K^+YN\pi$. In the counter experiment, the momentum spectra of K^+ mesons produced at 0° and 17° in the laboratory were obtained for incoming proton energies of 2.85 and 2.40 GeV. The 0° data show a narrow peak at the upper end of the K^+ momentum spectrum. It was speculated that this singularity could be caused by a bound state of the Λp system, a virtual system, or a resonant state.

In the present counter experiment, we have measured the momentum spectra of K^+ mesons produced at 20°, 30°, and 40° in the laboratory for incident proton energies of 2.54, 2.88, and 3.03 GeV. K^+ mesons, produced in a liquid-hydrogen target located inside the vacuum chamber of the Princeton-Pennsylvania accelerator (PPA), were identified by mass analysis.

* This work was supported by the U. S. Office of Naval Research Contract No. N0014-67-A-0151-0001.
† Present address: Lawrence Radiation Laboratory, University of California, Livermore, Calif.
[1] P. A. Piroué and A. J. S. Smith, Phys. Rev. **148**, 1315 (1966).
[2] P. A. Piroué, Phys. Letters **11**, 164 (1964). Due to an error in the beam calibration the *absolute* value of the K^+-meson cross sections reported in this paper are overestimated by a factor $\sim$6. This has, however, no bearing on the conclusions of the paper.
[3] R. L. Cool, T. W. Morris, R. R. Rau, A. M. Thorndike, and W. L. Whittemore, Phys. Rev. **108**, 1048 (1957); P. Baumel, G. Harris, J. Orear, and S. Taylor, *ibid.* **108**, 1322 (1957); D. Berley and G. B. Collins, *ibid.* **112**, 614 (1958).
[4] R. I. Louttit, T. W. Morris, D. C. Rahm, R. R. Rau, A. M. Thorndike, W. J. Willis, and R. M. Lea, Phys. Rev. **123**, 1465 (1961).
[5] A. C. Melissinos, N. W. Reay, J. T. Reed, T. Yamanouchi, E. Sacharidis, S. J. Lindenbaum, S. Ozaki, and L. C. L. Yuan, Phys. Rev. Letters **14**, 604 (1965).